Stability of Shell-Stiffened and Axisymmetrically Loaded Annular Plates

Dániel Burmeister

The present paper is concerned with the stability problems of a solid circular plate and some annular plates each stiffened by a cylindrical shell on the external boundary. Assuming an axisymmetric dead load and axisymmetric deformations we determine the critical load in order to clarify what effect the stiffening shell has on the critical load.

1 Introduction

In engineering practice we often meet structural elements loaded in their own plane like rods or plates. Because of their importance, stability problems of plates loaded in their own planes are an especially significant issue.

As regards the stability problems of circular plates, we mention that the first paper devoted to this question was published in 1890 (Bryan, 1890). It is also worth citing an article by Nádai (1915), who investigated some fundamental stability issues. Since then a number of papers have been devoted to the stability problems of circular plates but here we lay an emphasis only on those which deal with the influence of structural stiffening.

A structure can be stiffened in various ways. A solid circular plate (or an annular one) can be made more resistant to buckling by the use of a corrugation or by applying a stiffening along the diameter of the plate or by attaching a ring to the outer boundary of the plate or by making them more rigid with a cylindrical shell attached to the outer boundary of the plate.

Seeking in the scientific literature for papers devoted to the stability problem of stiffened annular plates we have come to the conclusion that there are only a few works dealing with this issue. A ring stiffened circular plate is investigated in a paper by Turvey and Der Avanessien (1989). The paper cited is concerned among others with experimental results. However, the stability issues are left out of consideration. A further paper by Turvey and Salehi (2008) deals with an annular plate stiffened by a single diameter stiffener. The stability problem is, however, again left out of consideration.

The influence of a stiffening ring attached between the two boundaries of the middle surface of circular plates on the stability is investigated by Frostig and Simitses (1988). It turns out from the references that the authors did not take into account the corresponding results of Szilassy (1971, 1976).

Szilassy investigated some stability problems of circular plates stiffened by a cylindrical shell on the outer boundary in (Szilassy, 1971, 1976). The main objective of his research was to clarify what effect the stiffening shell has on the critical load. If the stiffening significantly increases the buckling load than thin plates can be made more resistant against buckling by the application of a stiffening shell. The problems considered there include a boundary value problem for a solid circular plate and a few boundary value problems for annular plates. The author assumes that (i) the load is an in-plane axisymmetric dead one, and (ii) the deformations of the annular plate and the cylindrical shell are also axisymmetric. For the circular plates the author uses the solution of a differential equation set up for the rotation field – this choice excludes those boundary value problems from the set of solvable ones where a boundary condition is imposed on the deflection. As regards the cylindrical shell the solution is based on the theory of thin shells. After the investigations of Szilassy the following questions can be raised: (a) is it worth using a differential equation set up for the deflection in order to expand the range of solvable boundary value problems (the number of solvable problems can be increased in this way); (b) what is the influence of the shell height on the critical load; (c) is it worth investigating the case when the load is axisymmetric but the deformations due to the load are not; (d) what happens if the load is not axisymmetric.

The main objective of the present paper is to solve those boundary value problems which require the use of the differential equation set up for the deflection of the plate, i.e., where there is a boundary condition imposed on the deflection. The paper is organized in seven sections. Section 2 shortly outlines the physical problem to be solved. Section 3 presents the governing equations both for the circular plate and for the cylindrical shell. The stability problem of a solid circular plate is solved in Section 4. There we present both the non-linear equation which provides the critical load and the critical load for various shell heights. Section 5 is devoted to annular plates. First we shortly review the numerical method we use. Then we solve four different boundary value problems. Section 6 is a summary of the results. Appendix A includes some longer transformations.

As regards the possible applications we want to make the following remark. Assume that the inner space of a pressure vessel (a cylindrical shell) is separated into parts by annular plates. If the distance of the plates is above a certain limit and the buckling problem of the plates arises then the problem to be solved may coincide with the stability problem of a shell-stiffened annular plate provided that the shell height tends to infinity.

2 Problem Formulation

The cross section of the shell-stiffened structure we are concerned with is shown in Fig. 1. The structure consists of either a solid circular plate or an annular one – the latter is shown in Fig. 1 – and a cylindrical shell, which stiffens the plate on its external boundary. The inner radius of the plate is denoted by R_i, the radius of the intersection line of the middle surfaces of the plate and the shell by R_e. We shall assume that R_e coincides with the external radius of the plate. The thicknesses of the plate and shell are denoted by b_p and b_s, respectively. The shell is symmetric with respect to the middle plane of the plate. Its height is $2h$. The structure is loaded by radial distributed forces with a constant intensity f_o acting in the middle plane of the plate. The load is a dead one.
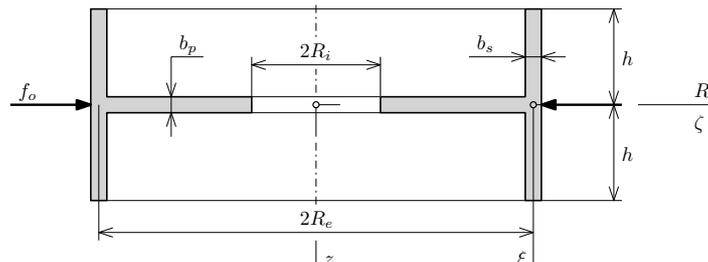
Figure 1: The structure and its load

We assume that the plate and the shell are thin, consequently we can use the Kirchhoff theory of plates and shells. It is also assumed that the problem is linear with regard to the kinematic equations and material law. Heat effects are not taken into account. The plate and the shell are made of the same homogeneous isotropic material for which $E = E_p = E_s$ and $\nu = \nu_p = \nu_s$ are Young's modulus and Poisson's ratio.
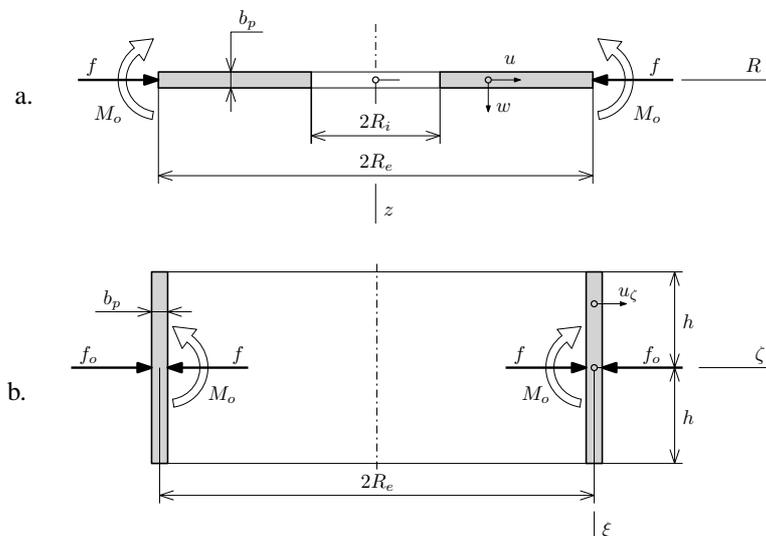
Figure 2: Free body diagram for plate and shell

Under the assumption of small, axisymmetric and linearly elastic deformations we determine (a) the critical load of the structure and (b) the effect of the stiffening shell on the critical load.

In order to solve the problem raised we separate the shell and plate from each other mentally. In accordance to this Figs. 2 a and b show the annular plate and the cylindrical shell one by one. The cylindrical coordinate system (R, φ, z) is used for the equations of the plate – the plane $z = 0$ coincides with the middle surface of the plate. Fig. 3 a shows the corresponding coordinate curves on the circle with radius R_e. The displacements on the middle surface in the directions R and z are denoted by u and w, respectively. The inner forces f and the bending moment M_o exerted by the cylindrical shell on the annular plate are also shown in Fig. 2.a.

For the cylindrical shell the coordinate system (ζ, φ, ξ) is applied. The coordinate surface $\xi = z$, $\zeta = 0$ coincides with the middle surface of the shell with radius R_e. The polar angle φ is the same in the two coordinate systems (due to the axisymmetry it plays, however, no role in the investigations). The coordinate curves on the middle surface of the shell are shown in Fig. 3 b.

a.   b.
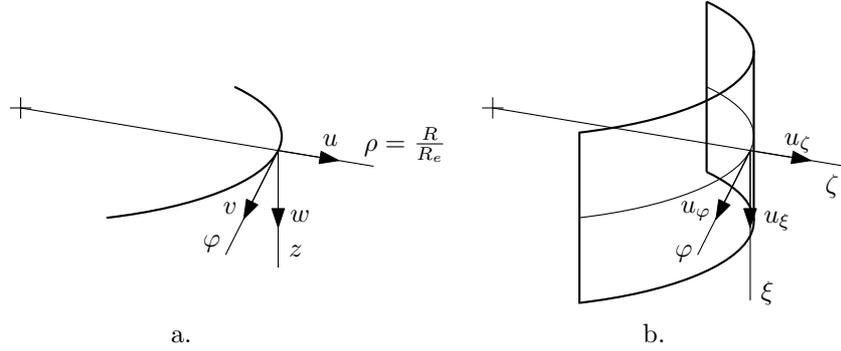
Figure 3: Coordinate curves in the coordinate systems

Assume that the deformations are axisymmetric and there is no load in the direction ξ on the shell. Then $u_\zeta = u_\zeta(\xi)$ is the only displacement component on the middle surface which is different from zero.

It is also obvious that $u = u(R)$, $w = w(R)$ and $u_\zeta = u_\zeta(\xi)$.

Fig. 2 b shows the inner forces f and the bending moment M_o exerted by the plate on the cylindrical shell.

3 Governing Equations

3.1 Governing Equations for the Cylindrical Shell

It is known that under the condition of axisymmetric deformations, the radial displacement u_ζ should satisfy the following differential equation (Timoshenko and Woinowski-Krieger, 1987, Chapter 15, p. 468)

$$\frac{\mathrm{d}^4 u_\zeta}{\mathrm{d}\xi^4} + 4\beta^4 u_\zeta = \frac{1}{I_{1s}E_{1s}}\left(-p - \nu\frac{N_\xi}{R_e}\right) \tag{1}$$

where p is the constant radial load exerted on the middle surface of the shell (its value is zero in the present case), N_ξ is the inner force in direction ξ (its value is zero as well), ν_s and E_s are Young's modulus and Poisson's ratio, respectively. In addition the following notations are introduced

$$\nu_o = \sqrt[4]{3(1 - \nu_s^2)}, \qquad\qquad \beta = \nu_o\sqrt{\frac{R_e}{b_s}}\frac{1}{R_e}, \tag{2a}$$

$$I_{1s} = b_s^3/12, \qquad\qquad E_{1s} = E_s/(1 - \nu_s^2). \tag{2b}$$

The shell shown in Fig. 2 b is subjected to the line loads f_o and f (as it has already been mentioned $p = 0$). There is also no load in the direction ξ on the shell. Consequently $N_\xi = 0$. The solution of equation (1) in the interval $\xi \in [0, h]$ takes the form

$$u_\zeta(\xi) = \sum_{i=1}^{4} a_i V_i(\beta\xi) + u_{\zeta\, p}; \quad u_{\zeta\, p} = -p/\beta^4 I_{1s}E_{1s} = 0, \tag{3}$$

where $V_i(\beta\xi)$ $(i = 1, \ldots, 4)$ denote the Krylov-functions – their definitions and derivatives are presented in the Appendix – see equations (53a) and (53b) for details.

The shear force and bending moment in the shell can be given in terms of u_ζ

$$Q_\zeta = I_{1s}E_{1s}\frac{\mathrm{d}^3 u_\zeta}{\mathrm{d}\xi^3} \qquad \text{and} \qquad M_\xi = -I_{1s}E_{1s}\frac{\mathrm{d}^2 u_\zeta}{\mathrm{d}\xi^2} \ . \tag{4}$$

The solution for u_ζ is a superposition of the solutions we determine for the following two partial loads

Load 1. The shell is subjected to the line loads f_o and f shown in Fig. 4 a The corresponding boundary conditions are as follows

$$Q_\zeta|_{\xi=0} = -\frac{f_o - f}{2} \ , \qquad\qquad \frac{\mathrm{d}u_\zeta}{\mathrm{d}\xi}\bigg|_{\xi=0} = 0 \ , \tag{5a}$$

$$Q_\zeta|_{\xi=h} = 0 \ , \qquad\qquad M_\xi|_{\xi=h} = 0 \ . \tag{5b}$$

Since $u_\zeta(\xi) = u_\zeta(-\xi)$ due to the load, the rotation about the axis φ is zero – cf. equation (5a)$_2$. The other boundary conditions are obvious.

Load 2. The shell is subjected to the couple system M_o shown in Fig. 4 b Now we have the following boundary conditions

$$u(\zeta)|_{\xi=0} = 0 \ , \qquad\qquad M_\xi|_{\xi=0} = -\frac{M_o}{2} \ , \tag{5c}$$

$$Q_\zeta|_{\xi=h} = 0 \ , \qquad\qquad M_\xi|_{\xi=h} = 0 \ . \tag{5d}$$

Observe that $u_\zeta(\xi) = -u_\zeta(-\xi)$ for this partial load. Consequently the displacement in the direction ζ should be zero at $\xi = 0$. The other boundary conditions are again obvious.
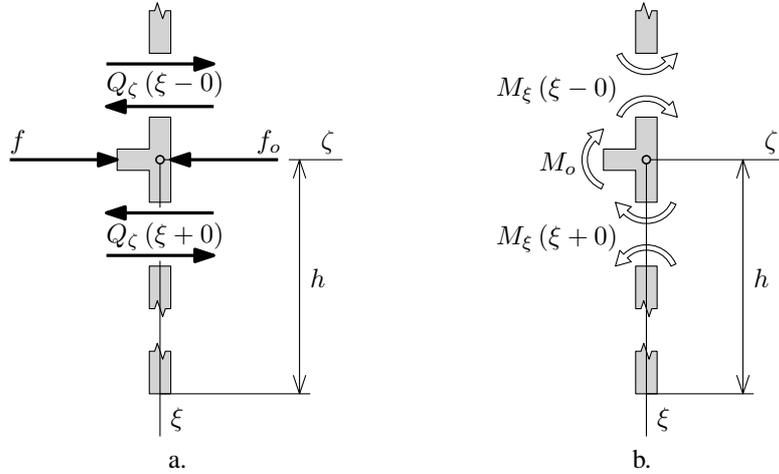
Figure 4: Partial loads of the shell

It follows from the symmetry of the problem that it is sufficient to determine the solution for the shell in the interval $\xi \in [0, h]$.

The solutions for the partial loads include the distributed force f and the bending moment M_o as unknown parameters. Theoretically, these quantities can be calculated from the continuity conditions. We prescribe the continuity conditions on the intersection line of the middle surfaces of the plate and the shell. Since $R = R_e$ and $\xi = 0$ on the intersection line, the kinematic quantities should satisfy the following continuity conditions

$$u\big|_{R=R_e} = u_o = u_{\zeta o} = u_\zeta\big|_{\xi=0} \tag{6a}$$

and

$$\vartheta_o = -\frac{\mathrm{d}w}{\mathrm{d}R}\bigg|_{R=R_e} = \frac{\mathrm{d}u_\zeta}{\mathrm{d}\xi}\bigg|_{\xi=0} \ . \tag{6b}$$

4

After some hand made calculations – see Sections 1.2. and 1.3 of the Appendix for details –, in which use has been made of the definitions of the Krylov-functions, we obtain

$$\vartheta_o = \left.\frac{\mathrm{d}u_\zeta}{\mathrm{d}\xi}\right|_{\xi=0} = \underbrace{-\frac{\nu_o^3}{E}\left(\frac{R_e}{b_s}\right)^{\frac{1}{2}}\frac{\cos 2h\beta + \cosh 2h\beta + 2}{\sinh 2h\beta - \sin 2h\beta}\frac{1}{b_s^2}}_{\kappa}M_o = -\kappa\,M_o\,. \tag{7a}$$

and

$$u_{\zeta o} = u_\zeta|_{\xi=0} = \underbrace{-\frac{\nu_o}{2E}\left(\frac{R_e}{b_s}\right)^{\frac{3}{2}}\frac{\cos 2h\beta + \cosh 2h\beta + 2}{\sin 2h\beta + \sinh 2h\beta}}_{\alpha}(f_o - f) = -\alpha\,(f_o - f)\,, \tag{7b}$$

where α and κ are defined by the above relations.

It follows from the continuity conditions (6) and relations (7) that the equations

$$\frac{\mathrm{d}w}{\mathrm{d}R} = \kappa\,M_o \qquad \text{and} \qquad u_o = -\alpha\,(f_o - f) \tag{8}$$

are satisfied. We shall see later that equation $(8)_1$ provides the value of f as non-linear equation and equation $(8)_2$ is to be used for calculating f_o.

3.2 Deformation of the Annular Plate, Governing Equations for the In-Plane Load

Under the assumption of axisymmetric deformations, the inner forces in the plate – we use the cylindrical coordinate system (R, φ, z) – due to the in-plane load exerted on the outer boundary are as follows

$$N_R = -A + \frac{B}{R^2}\,, \quad N_\varphi = -A - \frac{B}{R^2} \quad \text{and} \quad N_{R\varphi} = N_{\varphi R} = 0 \tag{9}$$

where the constants A and B depend on the boundary conditions. It follows from the axisymmetry that $N_{R\varphi}$ vanishes.

Let $\rho = R/R_e$ be a dimensionless coordinate. Further let $\rho_i = R_i/R_e$. It is clear that $\rho_i = 0$ for a solid circular plate.

If the inner boundary is free and f is the line load on the outer boundary – see Fig. 2 a – then the constants are as follows

$$A = f\frac{1}{1 - \rho_i^2} \qquad \text{and} \qquad B = f\frac{R_i^2}{1 - \rho_i^2}\,. \tag{10}$$

If the radial displacement vanishes on the inner boundary then

$$A = f\frac{1 + \nu}{1 + \nu + \rho_i^2(1 - \nu)} \quad \text{and} \quad B = -f\frac{R_i^2(1 - \nu)}{1 + \nu + \rho_i^2(1 - \nu)}\,. \tag{11}$$

If the plate is a solid one then

$$A = f \qquad \text{and} \qquad B = 0\,. \tag{12}$$

The radial displacement on the inner boundary can be calculated using the relations

$$u_o = -K\frac{R_e}{b_p}\frac{f}{E}\,, \tag{13}$$

where the constant K depends on the boundary condition

$$K = \frac{(1 - \nu)^2(1 - \rho_i^2)}{1 + \nu + \rho_i^2(1 - \nu)} \qquad\qquad \text{if} \qquad\qquad N_R|_{\rho=\rho_i} = 0\,, \tag{14}$$

$$K = \frac{(1 - \nu) + \rho_i^2(1 + \nu)}{1 + \rho_i^2} \qquad\qquad \text{if} \qquad\qquad u_o|_{\rho=\rho_i} = 0\,, \tag{15}$$

$$K = 1 - \nu \qquad\qquad \text{if} \qquad\qquad \rho_i = 0\,. \tag{16}$$

3.3 Deformation of the Annular Plate, Equations for the Displacement Field after Stability Loss

Let us introduce the notations

$$\mathcal{A} = \frac{A}{f} \; ; \qquad \mathcal{B} = \frac{B}{f} \; , \tag{17}$$

$$I_{1p} = b_p^3/12 \quad \text{and} \quad E_{1p} = E_p/(1 - \nu_p^2) \; . \tag{18}$$

Further let w be the displacement of the middle plane of the plate in the direction z – see Figure 3. Making use of the notations introduced one can show that w satisfies the differential equation

$$\Delta_H \Delta_H w = \frac{f}{I_{1p} E_{1p}} \left[\left(-\mathcal{A} + \frac{\mathcal{B}}{R^2} \right) \frac{\mathrm{d}^2 w}{\mathrm{d}R^2} + \left(-\mathcal{A} - \frac{\mathcal{B}}{R^2} \right) \frac{1}{R} \frac{\mathrm{d}w}{\mathrm{d}R} \right] \; , \tag{19a}$$

$$\Delta_H = \frac{\mathrm{d}^2}{\mathrm{d}R^2} + \frac{1}{R} \frac{\mathrm{d}}{\mathrm{d}R}$$

if the plate is an annular one. With regard to equations (12)

$$\Delta_H \Delta_H w = -\frac{f}{I_{1p} E_{1p}} \left[\frac{\mathrm{d}^2 w}{\mathrm{d}R^2} + \frac{1}{R} \frac{\mathrm{d}w}{\mathrm{d}R} \right] \tag{19b}$$

is the differential equation for w if the plate is solid. The rotation, the shear force and the bending moment can all be given in terms of the solution for w as follows

$$\vartheta = -\frac{\mathrm{d}w}{\mathrm{d}R} \; , \tag{20a}$$

$$M_R = -I_{1p} E_{1p} \left(\frac{\mathrm{d}^2 w}{\mathrm{d}R^2} + \nu \frac{1}{R} \frac{\mathrm{d}w}{\mathrm{d}R} \right) \; , \tag{20b}$$

$$Q_R = I_{1p} E_{1p} \frac{\mathrm{d}}{\mathrm{d}R} \left(\frac{\mathrm{d}^2 w}{\mathrm{d}R^2} + \frac{1}{R} \frac{\mathrm{d}w}{\mathrm{d}R} \right) - N_R \frac{\mathrm{d}w}{\mathrm{d}R} \; . \tag{20c}$$

4 Stability of the Shell-Stiffened Solid Circular Plate

4.1 Nonlinear Equation for the Critical Load

Introducing the notations

$$\mathfrak{F} = R_e^2 \frac{f}{I_{1p} E_{1p}} \qquad \text{and} \qquad \frac{1}{R_e^2} \tilde{\Delta} = \Delta_H = \frac{1}{R_e^2} \left(\frac{\mathrm{d}^2}{\mathrm{d}\rho^2} + \frac{1}{\rho} \frac{\mathrm{d}}{\mathrm{d}\rho} \right) \tag{21a}$$

in equation (19b) yields the differential equation

$$\tilde{\Delta} \tilde{\Delta} w + \mathfrak{F} \tilde{\Delta} w = 0 \; . \tag{21b}$$

Its solution takes the form

$$w(\rho) = c_1 Z_1 + c_2 Z_2 + c_3 Z_3 + c_4 Z_4 \; , \tag{22a}$$

$$Z_1 = 1 \; , \qquad Z_2 = \ln \rho \; , \qquad Z_3 = J_o(\sqrt{\mathfrak{F}}\rho) \; , \qquad Z_4 = Y_o(\sqrt{\mathfrak{F}}\rho) \tag{22b}$$

where c_i, $(i = 1, \ldots, 4)$ are undetermined constants of integration while Z_i denote the linearly independent particular solutions in which $J_n(\sqrt{\mathfrak{F}}\rho)$ and $Y_n(\sqrt{\mathfrak{F}}\rho)$, $n = 0, 1, 2, 3, \ldots$ are the Bessel functions of integer order.

For small values of $\sqrt{\mathfrak{F}}\rho$ the following asymptotic relation holds: $Y_o(\sqrt{\mathfrak{F}}\rho) \simeq \frac{2}{\pi} \ln(\sqrt{\mathfrak{F}}\rho)$. In addition $Z_3(0) = J_o(0) = 1$. Consequently the solution for w is limited if

$$c_2 = -2c_4/\pi \; . \tag{23}$$

Accordingly we get

$$w(\rho) = c_1 + c_4 \left[Y_o(\sqrt{\mathfrak{F}}\rho) - \frac{2}{\pi} \ln(\sqrt{\mathfrak{F}}\rho) \right] + c_3 J_o(\sqrt{\mathfrak{F}}\rho) \,. \tag{24}$$

By making use of the relations

$$\frac{2}{x} J_1(x) = J_2(x) + J_o(x) \qquad \text{and} \qquad \frac{2}{x} Y_1(x) = Y_2(x) + Y_o(x) \,, \tag{25}$$

the derivatives of Z_i from equations (70) and relation (20b) – the latter provides us the shear force – we obtain after some manipulations that

$$Q_R \frac{R_k^3}{I_1 E_1} = \frac{\mathrm{d}}{\mathrm{d}\rho} \left[\tilde{\Delta} + \mathfrak{F} \right] w = -c_4 \frac{2}{\pi} \mathfrak{F} \frac{1}{\rho} \,. \tag{26}$$

Since the shear force Q_R is zero on the circle with radius $R = \rho R_e$ if $\rho \to 0$, the previous equation yields

$$2\pi R \, Q_R = -4 c_4 f = 0 \,. \tag{27}$$

Consequently $c_4 = 0$. Therefore the solution for w is of the form

$$w(\rho) = c_1 + c_3 J_o(\sqrt{\mathfrak{F}}\rho) \,. \tag{28}$$

The remaining integration constants can be calculated from the boundary conditions prescribed at $\rho_i = 1$.

In what follows we assume that the thicknesses and the material of the cylindrical shell and the circular plate are the same. Thus $E_1 = E_{1s} = E_{1p}$, $\nu_s = \nu_p$, $b_s = b_p = b$ and $I_1 = I_{1s} = I_{1p}$.

According to equation (6)

$$\vartheta_o = -\kappa \, M_o \,. \tag{29}$$

The rotation at $R = R_e$ is of the form

$$\vartheta_o = -\left. \frac{\mathrm{d}w}{\mathrm{d}R} \right|_{R=R_e} = c_3 \frac{1}{R_e} \sqrt{\mathfrak{F}} J_1(\sqrt{\mathfrak{F}}) \,, \tag{30a}$$

where we have utilized relations (20a) and (70c)$_2$. Considering equation (19b), the properties of the solution and utilizing relations (70), which provides the derivatives of the Bessel functions, we obtain for the bending moment

$$M_o = -I_1 E_1 \left[\frac{\mathrm{d}^2 w}{\mathrm{d}R^2} + \nu \frac{1}{R} \frac{\mathrm{d}w}{\mathrm{d}R} \right]_{R=R_e} = -c_3 \frac{I_1 E_1}{R_e^2} \left[(1-\nu)\sqrt{\mathfrak{F}} J_1(\sqrt{\mathfrak{F}}) - \mathfrak{F} J_o(\sqrt{\mathfrak{F}}) \right] \,. \tag{30b}$$

Comparing equations (29) and (30) we get a non-linear equation for the critical load

$$\sqrt{\mathfrak{F}} J_1(\sqrt{\mathfrak{F}}) - \kappa \frac{I_1 E_1}{R_e} \left[(1-\nu)\sqrt{\mathfrak{F}} J_1(\sqrt{\mathfrak{F}}) - \mathfrak{F} J_o(\sqrt{\mathfrak{F}}) \right] = 0 \,. \tag{31}$$

This equation can be further transformed if we make use of relations (2a) and (2b) (the structural elements are of the same material and thickness) together with the definition of κ in equation (7a)

$$\sqrt{\mathfrak{F}} J_1(\sqrt{\mathfrak{F}}) - \frac{1}{12} \frac{\nu_o^3}{1-\nu^2} \sqrt{\frac{b}{R_e}} \frac{\cos 2h\beta + \cosh 2h\beta + 2}{\sinh 2h\beta - \sin 2h\beta} \left[(1-\nu) \frac{J_1(\sqrt{\mathfrak{F}})}{\sqrt{\mathfrak{F}}} - \mathfrak{F} J_o(\sqrt{\mathfrak{F}}) \right] = 0 \tag{32}$$

If we now take into account that $h\beta = \nu_o \sqrt{\frac{R_e}{b} \frac{h}{R_e}}$ we can conclude that the dimensionless critical load $\mathfrak{F}_{cr}$ – the corresponding value of f is denoted by f_{cr} – depends only on the dimensionless variables h/R_e and b/R_e for a fixed value of ν. In the sequel we assume that we have solved the above equation, i.e. we know the values of $\mathfrak{F}_{cr}$ and f_{cr}.

4.2 Results for a Solid Plate

In accordance with the notations introduced let $f_{o\,cr}$ be the critical value of f_o. A comparison of equations (7) and (13) yields

$$(1-\nu)\frac{R_e}{b}\frac{f_{cr}}{E} = \alpha(f_{o\,cr} - f_{cr})\,.$$

Consequently

$$\frac{f_{o\,cr}}{f_{cr}} = \frac{\mathfrak{F}_{o\,cr}}{\mathfrak{F}_{cr}} = 1 + 2\frac{1-\nu}{\nu_o}\sqrt{\frac{R_e}{b}}\frac{\cos 2h\beta + \cosh 2h\beta + 2}{\sinh 2h\beta - \sin 2h\beta}\,, \quad \mathfrak{F}_{o\,cr} = R_e^2\frac{f_{o\,cr}}{I_{1p}E_{1p}}\,. \tag{33}$$

Clearly the quotient $\frac{f_{o\,cr}}{f_{cr}} = \frac{\mathfrak{F}_{o\,cr}}{\mathfrak{F}_{cr}}$ depends also on the dimensionless variables h/R_e and b/R_e for a fixed value of ν. This function is presented in Fig. 5.
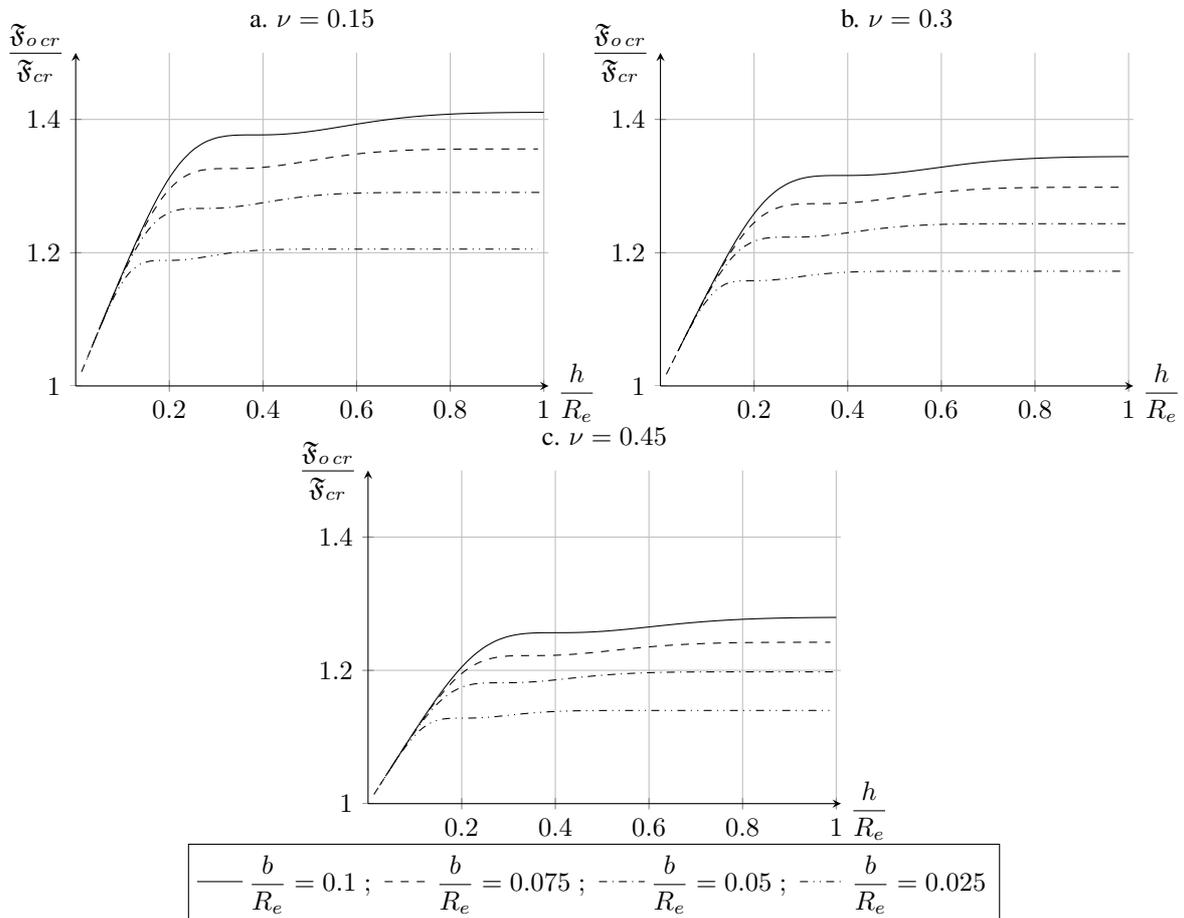
Figure 5: Quotient $\mathfrak{F}_{o\,cr}/\mathfrak{F}_{cr}$ against h/R_e for some values of b/R_e and ν

We introduce the following notations for the critical load and the dimensionless critical load if there is no stiffening shell

$$f_{o\,cr}\,(h=0) = f_{of\,cr} \quad \text{and} \quad \mathfrak{F}_{o\,cr}\,(h=0) = \mathfrak{F}_{of\,cr}\,. \tag{34}$$

It is again obvious that the quotient of the critical loads (or which is the same that of the dimensionless critical loads) for a given ν

$$\frac{f_{o\,cr}}{f_{of\,cr}} = \frac{\mathfrak{F}_{o\,cr}}{\mathfrak{F}_{of\,cr}} \tag{35}$$

depends only on h/R_e and b/R_e, which, in the sequel, are referred to as dimensionless height and thickness.

A code has been written in Fortran 90 to solve the non-linear equation (32) for $\mathfrak{F}_{cr}$ and compute $f_{o\,cr}$, $f_{of\,cr}$, and $\mathfrak{F}_{o\,cr}$, $\mathfrak{F}_{of\,cr}$. The computational results are presented in Fig. 6 for $\nu = 0.15,\ 0.3$ and 0.45. It is clear from the graphs that the height of the plate does not affect the critical load if the height is larger than a certain value.
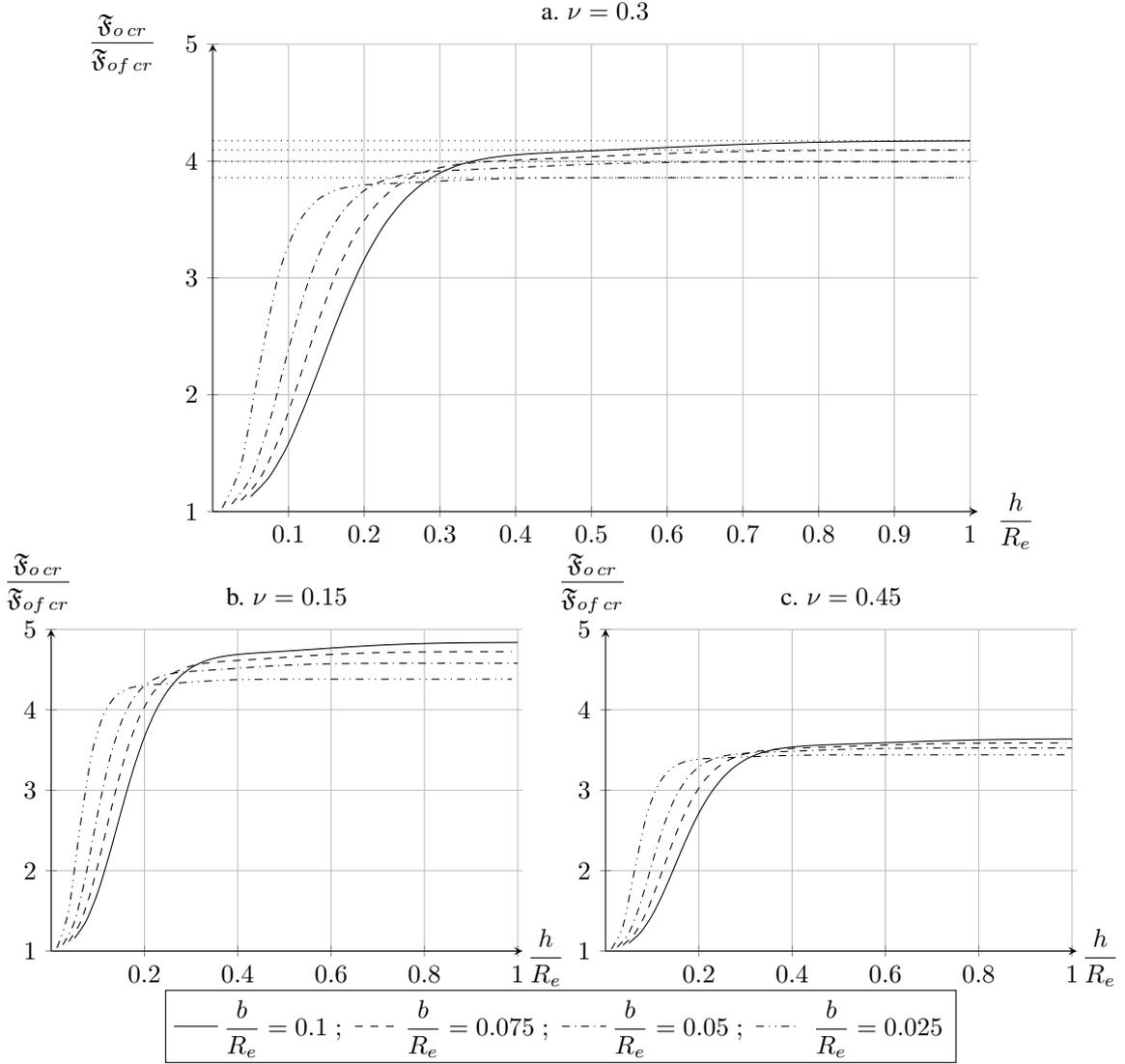
Figure 6: $f_{o\,cr}/f_{oh\,cr}$ against h/R_e for some b/R_e; $\nu = 0.15,\ 0.3,\ 0.45$

It follows from equations (7) that the stiffening shell can be replaced by a tension spring and a torsion spring on its outer diameter. The corresponding arrangement is shown in Fig. 7.
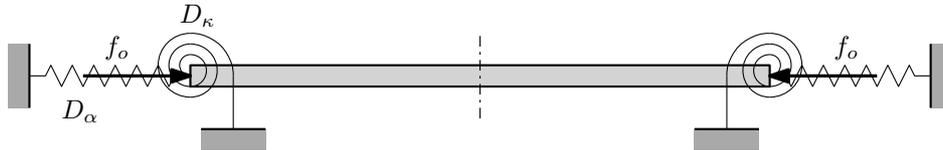
Figure 7: Spring model

Hooke's law for these springs (tension and torsion) takes the form

$$f_o - f = -D_\alpha u_{\zeta o}\ , \qquad M_o = -D_\kappa \vartheta_o \tag{36}$$

where $D_\alpha = \frac{1}{\alpha}$ and $D_\kappa = \frac{1}{\kappa}$ are the spring constants.

If the height h of the shell tends to infinity the terms α and κ are limited. Consequently the critical load is limited

as well. The limits of the critical loads belong to the values

$$\lim_{h\to\infty} \alpha = \lim_{h\to\infty} \frac{\nu_o}{2E} \left(\frac{R_e}{b_s}\right)^{\frac{3}{2}} \frac{\cos 2h\beta + \cosh 2h\beta + 2}{\sin 2h\beta + \sinh 2h\beta} = \frac{\nu_o}{2E} \left(\frac{R_e}{b_s}\right)^{\frac{3}{2}}, \tag{37}$$

$$\lim_{h\to\infty} \kappa = \lim_{h\to\infty} \frac{\nu_o^3}{E} \left(\frac{R_e}{b_s}\right)^{\frac{1}{2}} \frac{\cos 2h\beta + \cosh 2h\beta + 2}{\sinh 2h\beta - \sin 2h\beta} \frac{1}{b_s^2} = \frac{\nu_o^3}{E} \left(\frac{R_e}{b_s}\right)^{\frac{1}{2}} \frac{1}{b_s^2}. \tag{38}$$

These limits are presented with horizontal lines in the upper graph in Fig. 6.

5 Stability of the Shell-Stiffened Annular Plates

5.1 A Numerical Procedure to Determine the Critical Load

Equation (19a) has no closed form solution. For this reason we develop a numerical algorithm for the solution of the eigenvalue problem defined by equation (19a) and the corresponding boundary conditions. First we rewrite equation (19a) in the form

$$\frac{\mathrm{d}^4 w}{\mathrm{d}\rho^4} = F\left(\frac{\mathrm{d}^3 w}{\mathrm{d}\rho^3}, \frac{\mathrm{d}^2 w}{\mathrm{d}\rho^2}, \frac{\mathrm{d}w}{\mathrm{d}\rho}, w, \mathfrak{F}, \rho\right) =$$
$$= -\frac{2}{\rho} \frac{\mathrm{d}^3 w}{\mathrm{d}\rho^3} + \frac{1}{\rho^2} \frac{\mathrm{d}^2 w}{\mathrm{d}\rho^2} - \frac{1}{\rho^3} \frac{\mathrm{d}w}{\mathrm{d}\rho} + \mathfrak{F}\left[\left(-\mathcal{A} + \frac{\mathcal{B}R_e^2}{\rho^2}\right) \frac{\mathrm{d}^2 w}{\mathrm{d}\rho^2} + \left(-\mathcal{A} - \frac{\mathcal{B}R_e^2}{\rho^2}\right) \frac{1}{\rho} \frac{\mathrm{d}w}{\mathrm{d}\rho}\right] \tag{39}$$

and then we replace this ordinary differential equation of order four by a system of differential equations of order one. To this end we introduce appropriately defined new intermediate variables p, q and s by the use of which we obtain

$$\frac{\mathrm{d}w}{\mathrm{d}\rho} = p, \quad \frac{\mathrm{d}p}{\mathrm{d}\rho} = q, \quad \frac{\mathrm{d}q}{\mathrm{d}\rho} = s, \quad \frac{\mathrm{d}s}{\mathrm{d}\rho} = F(s, q, p, w, \mathfrak{F}, \rho). \tag{40a}$$

where

$$F = -\frac{2s}{\rho} + \frac{q}{\rho^2} - \frac{p}{\rho^3} + \mathfrak{F}\left(\left(-\mathcal{A} + \frac{\mathcal{B}R_e^2}{\rho^2}\right) q + \left(-\mathcal{A} - \frac{\mathcal{B}R_e^2}{\rho^2}\right) \frac{p}{\rho}\right). \tag{40b}$$

Variables w, p, q and s constitute a column matrix

$$\mathbf{u}^T(\rho) = \begin{bmatrix} w & p & q & s \end{bmatrix} \tag{41}$$

where the superscript T stands for the transpose of a matrix. It is clear that $\mathbf{u}$ fulfills the matrix equation

$$\frac{\mathrm{d}\mathbf{u}}{\mathrm{d}\rho} = \begin{bmatrix} p \mid q \mid q \mid F(s, q, p, w, F, \rho) \end{bmatrix}^T. \tag{42}$$

We seek solutions in the interval $\rho \in [\rho_i, 1]$. It is easy to see that the particular solutions
$$\mathbf{u}_k = \begin{bmatrix} u_{1k} \mid u_{2k} \mid u_{3k} \mid u_{4k} \end{bmatrix}^T \qquad (k = 1, 2, 3, 4)$$
are linearly independent if they satisfy the following initial conditions

$$\mathbf{u}_1|_{\rho_i} = \begin{bmatrix} 1 \\ 0 \\ 0 \\ 0 \end{bmatrix}, \quad \mathbf{u}_2|_{\rho_i} = \begin{bmatrix} 0 \\ 1 \\ 0 \\ 0 \end{bmatrix}, \quad \mathbf{u}_3|_{\rho_i} = \begin{bmatrix} 0 \\ 0 \\ 1 \\ 0 \end{bmatrix}, \quad \mathbf{u}_4|_{\rho_i} = \begin{bmatrix} 0 \\ 0 \\ 0 \\ 1 \end{bmatrix} \tag{43}$$

Consequently the solution of equation (42) assumes the form

$$\mathbf{u} = C_1 \mathbf{u}_1 + C_2 \mathbf{u}_2 + C_3 \mathbf{u}_3 + C_4 \mathbf{u}_4, \tag{44}$$

where $C_1, \dots, C_2$ are constants of integration.

Differential equations (42) are associated with homogenous boundary conditions on the inner boundary $\rho = \rho_i$ and also on outer boundary $\rho = \rho_e = 1$. We shall detail the boundary conditions when we present the solution for the various support arrangements. At this point we remark that the differential equation (42) and the homogenous

10

boundary conditions together define the eigenvalue problem which provides the dimensionless eigenvalue $\mathfrak{F}$ for a given support arrangement of the structure consisting of a shell and an annular plate.

Every physical quantity can be given in terms of the particular solutions $\mathbf{u}_1, \ldots, \mathbf{u}_4$. On the basis of relations (40) and (20) we obtain the displacement field

$$w(\rho) = C_1 u_{11} + C_2 u_{12} + C_3 u_{13} + C_4 u_{14} \,, \tag{45a}$$

the rotation field

$$\vartheta = \frac{1}{R_e} \frac{dw}{d\rho} = \frac{1}{R_e} \left(C_1 u_{21} + C_2 u_{22} + C_3 u_{23} + C_4 u_{24} \right) \,, \tag{45b}$$

the bending moment

$$M_R = -\frac{I_1 E_1}{R_k^2} \left[\left(u_{31} + \frac{\nu}{\rho} u_{21} \right) C_1 + \left(u_{32} + \frac{\nu}{\rho} u_{22} \right) C_2 + \right.$$
$$\left. + \left(u_{33} + \frac{\nu}{\rho} u_{23} \right) C_3 + \left(u_{34} + \frac{\nu}{\rho} u_{24} \right) C_4 \right] \,, \tag{45c}$$

and the shear force

$$Q_R = \frac{I_1 E_1}{R_e^3} \left\{ \left[u_{41} + \frac{1}{\rho} u_{31} + \left(\mathfrak{F} - \frac{1}{\rho^2} \right) u_{21} \right] C_1 + \left[u_{42} + \frac{1}{\rho} u_{32} + \left(\mathfrak{F} - \frac{1}{\rho^2} \right) u_{22} \right] C_2 + \right.$$
$$\left. + \left[u_{43} + \frac{1}{u\,33} (\rho) + \left(\mathfrak{F} - \frac{1}{\rho^2} \right) u_{23} \right] C_3 + \left[u_{44} + \frac{1}{\rho} u_{34}(\rho) + \left(\mathfrak{F} - \frac{1}{\rho^2} \right) u_{24} \right] C_4 \right\} \,. \tag{45d}$$

Finally we remark that the solutions $\mathbf{u}_1, \ldots, \mathbf{u}_4$ are computed using an adaptive fourth-order Runge-Kutta method.

5.2 Comparison with the Solution Valid for the Solid Plate

We have tested the numerical algorithm described above by solving the problem of the solid circular plate again. The corresponding boundary conditions are in principle the same as before

$$\lim_{\rho \longrightarrow 0} w = \text{finite} \,, \quad \left. \frac{dw}{d\rho} \right|_{\rho=0} = 0 \,, \tag{46}$$

$$\left. \frac{dw}{d\rho} \right|_{\rho=1} = -\frac{1}{12} \frac{\nu_o^3}{1 - \nu^2} \sqrt{\frac{b}{R_e}} \frac{\cos 2h\beta + \cosh 2h\beta + 2}{\sinh 2h\beta - \sin 2h\beta} \left. \left(\frac{d^2 w}{d\rho^2} + \frac{\upsilon}{\rho} \frac{dw}{d\rho} \right) \right|_{\rho=1} \tag{47}$$

$$\left. \frac{d}{d\rho} \left[\frac{d^2}{d\rho^2} + \frac{1}{\rho} \frac{d}{d\rho} + \mathfrak{F} \right] w \right|_{\rho=0+\varepsilon} = 0 \,. \tag{48}$$

The displacement of the plate at $\rho = 0$ is $u_{11} = C_1$. It does not violate generality if we set this value to zero – it is actually the rigid body motion of the structure in the vertical direction. If $C_1 = 0$ the three boundary conditions left yield the following homogenous linear system of equations

$$C_2 u_{22}(0) + C_3 u_{23}(0) + C_4 u_{24}(0) = 0 \tag{49a}$$

$$C_2 \left[-\kappa \frac{I_1 E_1}{R_k} \left(u_{32}(1) + \nu u_{22}(1) \right) - u_{22}(1) \right] + C_3 \left[-\kappa \frac{I_1 E_1}{R_e} \left(u_{33}(1) + \nu u_{23}(1) \right) - u_{23}(1) \right] +$$
$$+ C_4 \left[-\kappa \frac{I_1 E_1}{R_e} \left(u_{34}(1) + \nu u_{24}(1) \right) - u_{24}(1) \right] = 0 \tag{49b}$$

$$\left\{ C_2 \left[u_{42}(\rho) + \frac{1}{\rho} u_{32}(\rho) + \left(\mathfrak{F} - \frac{1}{\rho^2} \right) u_{22}(\rho) \right] + \right.$$
$$+ C_3 \left[u_{43}(\rho) + \frac{1}{\rho} u_{33}(\rho) + \left(\mathfrak{F} - \frac{1}{\rho^2} \right) u_{23}(\rho) \right] +$$
$$\left. + C_4 \left[u_{44}(\rho) + \frac{1}{\rho} u_{34}(\rho) + \left(\mathfrak{F} - \frac{1}{\rho^2} \right) u_{24}(\rho) \right] \right\} \bigg|_{\rho=0+\varepsilon} = 0 \,, \tag{49c}$$

11

with C_2, C_3 and C_4 as unknowns. This equation system has a non-trivial solution if the determinant of the coefficient matrix vanishes

$$D(\mathfrak{F}) = \begin{vmatrix} u_{22}(0) & u_{23}(0) & u_{24}(0) \\ -\kappa\frac{I_1 E_1}{R_k}\left(u_{32}(1) + \nu u_{22}(1)\right) & -\kappa\frac{I_1 E_1}{R_k}\left(u_{33}(1) + \nu u_{23}(1)\right) & -\kappa\frac{I_1 E_1}{R_k}\left(u_{34}(1) + \nu u_{24}(1)\right) \\ -u_{22}(1)) & -u_{23}(1) & -u_{24}(1) \\ \left\{u_{42}(\rho) + \frac{1}{\rho}u_{32}(\rho) + \right. & \left\{u_{43}(\rho) + \frac{1}{\rho}u_{33}(\rho) + \right. & \left\{u_{44}(\rho) + \frac{1}{\rho}u_{34}(\rho) + \right. \\ \left. + \left(\mathfrak{F} - \frac{1}{\rho^2}\right)u_{22}(\rho)\right\}\Big|_{\rho=0+\varepsilon} & \left. + \left(\mathfrak{F} - \frac{1}{\rho^2}\right)u_{23}(\rho)\right\}\Big|_{\rho=0+\varepsilon} & \left. + \left(\mathfrak{F} - \frac{1}{\rho^2}\right)u_{24}(\rho)\right\}\Big|_{\rho=0+\varepsilon} \end{vmatrix} = 0 \quad (50)$$

Fig. 8. shows the critical load obtained by using the two methods: (a) solution of equation (32) (b) solution by the use of the Runge-Kutta procedure.

Figure 8: analytic-numeric comparison

We have carried out the computations under the assumption that $b/R_e = 0.05$, $E = 2.1 \times 10^5$ N/mm^2 and $\nu = 0.3$. It is clear from Fig. 8 that the two curves coincide basically with each other. It is worth noting again that the dimensionless load $\mathfrak{F}$ as well as the quotient $\frac{f_{o\,cr}}{f_{oh\,cr}}$ depend only on h/R_e and b/R_e both for the sold circular plate and for the annular plates if ν and ρ_i have fixed values.

5.3 Results for Annular Plates

In the present section we determine the critical loads for four different support arrangements. The solutions are presented in the subsections 5.3.1., 5.3.2., 5.3.3. and 5.3.4.

5.3.1 Simple Supported Plate

First we shall investigate a shell-stiffened annular plate with a simple support on its inner boundary. Since the radial displacement is not prescribed on the inner boundary it follows that the boundary condition $N_R|_{\rho=\rho_i} = 0$ must be satisfied there. The whole structure is presented in Fig. 9. We remark that the values of $\mathcal{A}$ and $\mathcal{B}$ in equation (39), which provides the critical value of $\mathcal{F}$, are computed from relations (10) and (17). Furthermore we also remark that K can be obtained from relation (14) when we calculate u_o using equation (13).

12

Figure 9: Simple support on the inner boundary
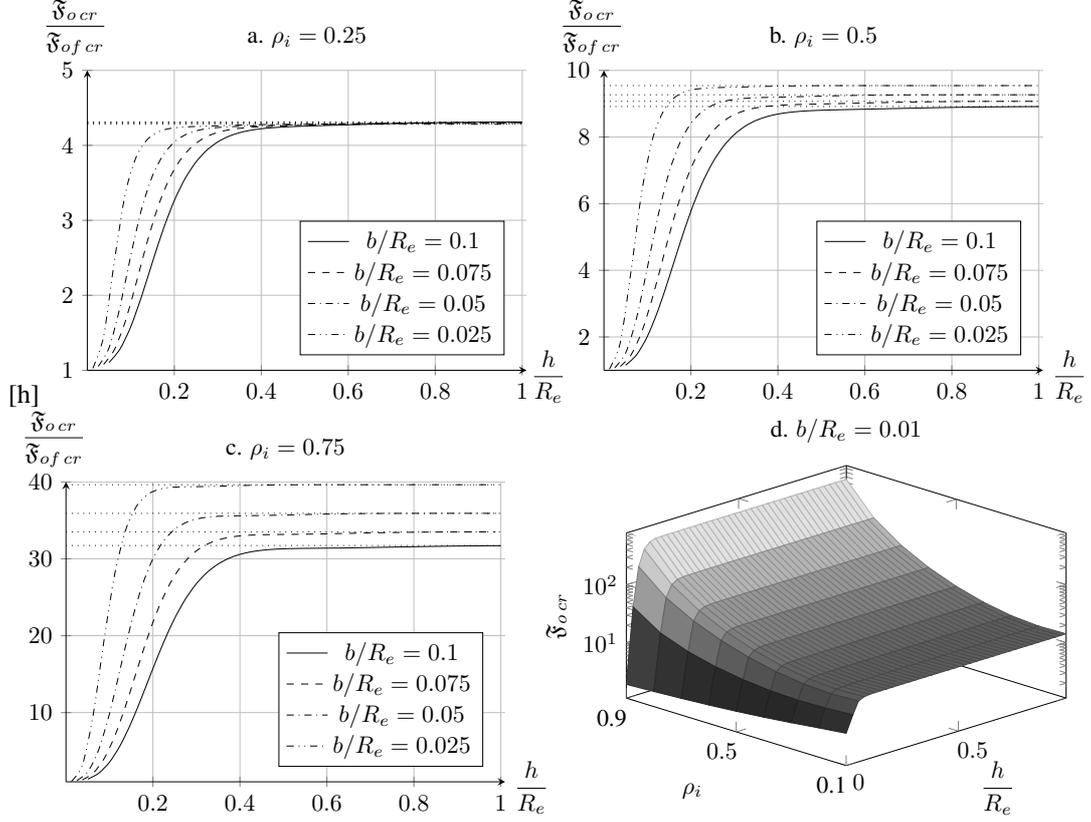
Figure 10 a-c: Quotient of the dimensionless critical loads as a function of the dimensionless
height and thickness for the structure shown in Fig. 9 if $\rho = 0.25$, $\rho = 0.5$, $\rho = 0.75$
d: Dimensionless critical load as a function of ρ_i and the dimensionless shell height

The solution w of the plate equation (19a) (or the solutions of the differential equations (42)) should fulfill the following boundary conditions

$$w|_{\rho=\rho_i} = 0\,, \qquad \frac{\mathrm{d}^2 w}{\mathrm{d}\rho^2} + \frac{\nu}{\rho}\frac{\mathrm{d}w}{\mathrm{d}\rho}\bigg|_{\rho=\rho_i} = 0 \tag{51a}$$

$$\frac{\mathrm{d}w}{\mathrm{d}\rho}\bigg|_{\rho=1} = -\frac{1}{12}\frac{\nu_o^3}{1-\nu^2}\sqrt{\frac{b}{R_e}}\,\frac{\cos 2h\beta + \cosh 2h\beta + 2}{\sinh 2h\beta - \sin 2h\beta}\left(\frac{\mathrm{d}^2 w}{\mathrm{d}\rho^2} + \frac{\upsilon}{\rho}\frac{\mathrm{d}w}{\mathrm{d}\rho}\right)\bigg|_{\rho=1} \tag{51b}$$

$$\frac{\mathrm{d}}{\mathrm{d}\rho}\left[\frac{\mathrm{d}^2}{\mathrm{d}\rho^2} + \frac{1}{\rho}\frac{\mathrm{d}}{\mathrm{d}\rho} + \mathfrak{F}\right]w\bigg|_{\rho=1} = 0\,. \tag{51c}$$

The computational results are shown in Fig. 10 a-c for three different values of ρ_i. Fig. 10 d shows the critical load of a specific structure ($E = 2.1 \times 10^5$ N/mm^2, $\nu = 0.3$) against ρ_i and h/R_e in a three-dimensional graph for the fixed value $b/R_e = 0.01$. The axis $\mathfrak{F}_{o\,cr}$ is a logarithmic one in this part of the figure.

5.3.2 Annular Plate with Clamped Inner Boundary

If (a) the radial displacement is not prescribed on the inner boundary but (b) the rotation is zero (in contrast to the previous problem) – see Fig. 11 for further details –

13
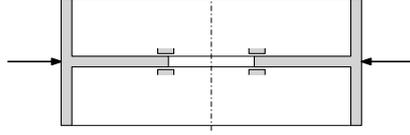
Figure 11: Shell and plate clamped on the inner boundary
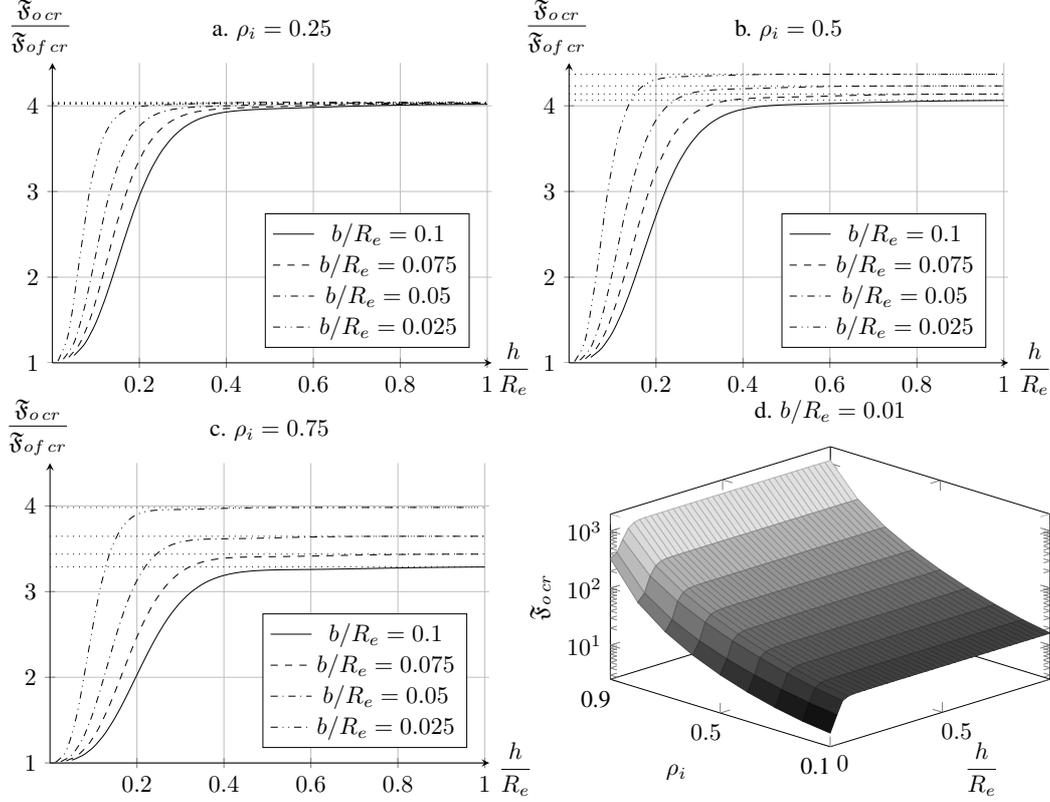
Figure 12 a-c: Quotient of the dimensionless critical loads as a function of the dimensionless
height and thickness for the structure shown in Fig. 11 if $\rho = 0.25$, $\rho = 0.5$, $\rho = 0.75$
d: Dimensionless critical load as a function of ρ_i and the dimensionless shell height

then the equation

$$\frac{\mathrm{d}w}{\mathrm{d}\rho}\bigg|_{\rho=\rho_i} = 0 \; , \tag{52}$$

together with equations (51a)$_1$, (51b) and (51c) are the boundary conditions. The effect of the stiffening to the
structure shown in Fig. 11 can be seen in Fig. 12 a-c.

We remark that Fig. 12 d shows again the critical load against ρ_i and h/R_e in a three-dimensional graph for a
specific structure (the parameters are the same as those of the structure in Fig. 9). The vertical axis is logarithmic
as well.

5.3.3 Axially and Radially Supported Annular Plate

If (a) the radial displacement on the inner boundary of the plate is zero, i.e. $u_o|_{\rho=\rho_i} = 0$ then the values of $\mathcal{A}$ and
$\mathcal{B}$ in equation (39), which provides the critical value of $\mathcal{F}$, should be computed from relations (11) and (17). We
also remark that K can be obtained from relation (15) when we calculate u_o using equation (13). Furthermore if
the plate is simply supported on its inner boundary then the corresponding boundary conditions are the same as
those given by equation (51).
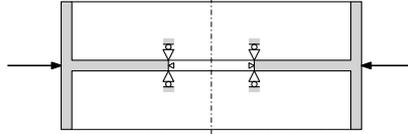
Figure 13: Simple supported plate with no radial displacement on the inner boundary

Fig. 15 a shows again the critical load against ρ_i and h/R_e in a three-dimensional graph for a specific structure (the parameters are the same as those of the previous two problems). The vertical axis is logarithmic as well.

5.3.4 Annular Plate Fixed on the Inner Boundary

If the displacements and the rotation are zero on the inner boundary – the structure is shown in Fig. 14 – then the only difference between this problem and the previous one is that boundary condition (52) should be applied instead of boundary condition (51a)$_2$.
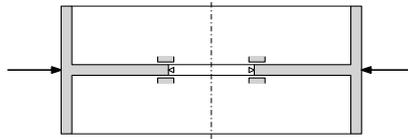
Figure 14: Plate fixed on the inner boundary

In accordance with the Figures that have been already presented before Fig. 15 b shows the critical load against ρ_i and h/R_e in a three-dimensional graph for a specific structure – the parameters of which are also the same as earlier. The vertical axis is again a logarithmic one.
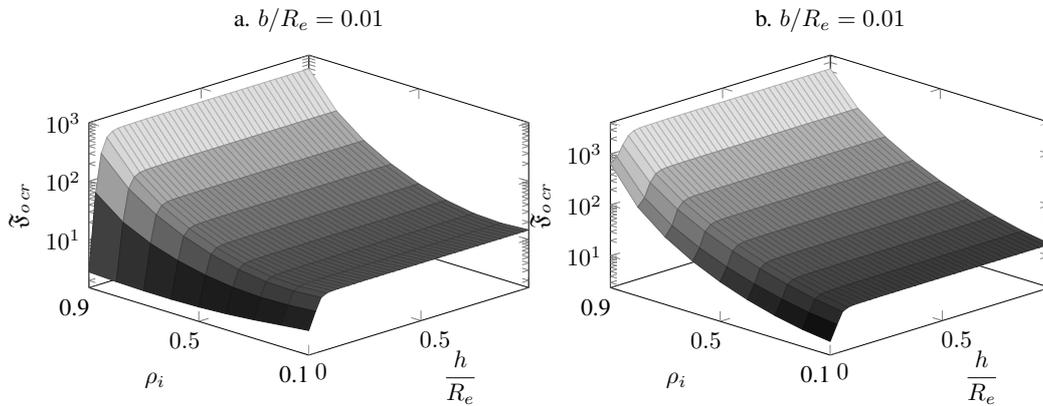
Figure 15 a-b: Dimensionless critical load as a function of ρ_i and the dimensionless shell height for the structures shown in Fig. 13 and Fig. 14

6 Concluding Remarks

In accordance with the objectives in the introduction we have summed up the differential equations for the stability problem of solid circular plates and annular plates under the assumption of axisymmetric deformations. In addition we have clarified what the continuity conditions are between the plate and the cylindrical shell which stiffens the plate. We have established the nonlinear equations which provide the critical load. We have also developed a procedure for computing numerical solutions. One of these can be used for the solid circular plate the other for annular plates. We have coded the procedure in Fortran 90 and made computations in order to determine the critical load.

Solutions are provided for a solid circular plate and for four support types concerning the annular plates. According to the results obtained the stiffening shell increases the value of critical load significantly if the quotient h/R_e does not exceed a limit the value of which depends on b/R_e and ρ_i.

Recalling the introduction we finally remark that (i) it is an interesting question what happens if the load is axisymmetric but the deformations due to it are not, and (ii) what happens if the load is also non-axisymmetric. Partial results for problem (i) are presented in a conference proceeding (Burmeister, 2011).

7 Acknowledgement

A Solution of Partial Problems

1.1 Krylov-Functions

For completeness we present the Krylov-functions together with their derivatives with respect to the coordinate ξ below:

$$V_1 = \cosh \beta \xi \cos \beta \xi \,, \qquad V_2 = \frac{1}{2} \left(\cosh \beta \xi \sin \beta \xi + \sinh \beta z \cos \beta \xi \right) \,,$$
$$V_3 = \frac{1}{2} \sinh \beta \xi \sin \beta \xi \,, \quad V_4 = \frac{1}{4} \left(\cosh \beta \xi \sin \beta \xi - \sinh \beta z \cos \beta \xi \right) \,. \tag{53a}$$

$$
\begin{array}{llll}
V_1' = -4\beta V_4 \,, & V_2' = \beta V_1 \,, & V_3' = \beta V_2, & V_4' = \beta V_3 \,, \\
V_1'' = -4\beta^2 V_3 \,, & V_2'' = -4\beta^2 V_4 \,, & V_3'' = \beta^2 V_1 \,, & V_4'' = \beta^2 V_2 \,, \\
V_1''' = -4\beta^3 V_2 \,, & V_2''' = -4\beta^3 V_3 \,, & V_3''' = -4\beta^3 V_4, & V_4''' = \beta^3 V_1 \,.
\end{array}
\tag{53b}
$$

1.2 Solution for the First Partial Load

On the basis of equations (3) and (53b) we take into account in our calculations that the following relations are valid for the solutions of differential equation (1) and its derivatives

$$
\begin{aligned}
u_\zeta &= a_1 V_1 + a_2 V_2 + a_3 V_3 + a_4 V_4 \\
u_\zeta' &= -4\beta a_1 V_4 + \beta a_2 V_1 + \beta a_3 V_2 + \beta a_4 V_3 \\
u_\zeta'' &= -4\beta^2 a_1 V_3 - 4\beta^2 a_2 V_4 + \beta^2 a_3 V_1 + \beta^2 a_4 V_2 \\
u_\zeta''' &= -4\beta^3 a_1 V_2 - 4\beta^3 a_2 V_3 - 4\beta^3 a_3 V_4 + \beta^3 a_4 V_1 \,.
\end{aligned}
\tag{54}
$$

For the sake of our later considerations it is worth introducing the notations

$$
\begin{aligned}
V_{1h} &= V_1(\xi = h) = \cosh \beta h \cos \beta h \\
V_{2h} &= V_2(\xi = h) = \frac{1}{2} \left(\cosh \beta h \sin \beta h + \sinh \beta h \cos \beta h \right) \\
V_{3h} &= V_3(\xi = h) = \frac{1}{2} \sinh \beta h \sin \beta h \\
V_{4h} &= V_4(\xi = h) = \frac{1}{4} \left(\cosh \beta h \sin \beta h - \sinh \beta h \cos \beta h \right) \,.
\end{aligned}
\tag{55}
$$

Boundary condition (5a)$_2$ yields

$$u_\zeta'|_{\xi=0} = \beta a_2 = 0 \qquad \text{therefore} \qquad a_2 = 0 \,. \tag{56}$$

Similarly we obtain from a comparison of the boundary condition (5a)$_1$ and relation (4)$_1$

$$I_{1s} E_{1s} u_\zeta'''|_{\xi=0} = I_{1s} E_{1s} \beta^3 a_4 = -\frac{f_o - f}{2} \,, \quad \text{therefore} \quad a_4 = -\frac{f_o - f}{2} \frac{1}{I_{1s} E_{1s}} \frac{1}{\beta^3} \,. \tag{57}$$

On the basis of boundary conditions (5b)$_{1,2}$ and (4) we obtain the linear system of equations

$$u_\zeta'''|_{\xi=h} = -4\beta^3 a_1 V_{2h} - 4\beta^3 a_3 V_{4h} - \beta^3 \frac{f_o - f}{2} \frac{1}{I_{1s} E_{1s}} \frac{1}{\beta^3} V_{1h} = 0 \,,$$
$$u_\zeta''|_{\xi=h} = 4\beta^2 a_1 V_{3h} - \beta^2 a_3 V_{1h} + \beta^2 \frac{f_o - f}{2} \frac{1}{I_{1s} E_{1s}} \frac{1}{\beta^3} V_{2h} = 0 \tag{58}$$

to calculate the two integration constants left. Substituting the solution

$$\begin{bmatrix} a_1 \\ a_3 \end{bmatrix} = -\frac{f_o - f}{2} \frac{1}{I_{1s}E_{1s}} \frac{1}{\beta^3} \begin{bmatrix} \dfrac{(V_{1h}^2 + 4V_{2h}V_{4h})}{4V_{1h}V_{2h} + 16V_{3h}V_{4h}} \\ \dfrac{V_{1h}V_{3h} - V_{2h}^2}{V_{1h}V_{2h} + 4V_{3h}V_{4h}} \end{bmatrix} \tag{59}$$

and the other two integration constants into $(54)_1$ we have

$$u_\zeta = \frac{f_o - f}{2} \frac{1}{I_{1s}E_{1s}} \frac{1}{\beta^3} \left(-\frac{V_{1h}^2 + 4V_{2h}V_{4h}}{4V_{1h}V_{2h} + 16V_{3h}V_{4h}} V_1 + \frac{V_{2h}^2 - V_{1h}V_{3h}}{V_{1h}V_{2h} - 4V_{3h}V_{4h}} V_3 - V_4 \right) , \tag{60}$$

from where

$$u_\zeta(\xi = 0) = -\frac{f_o - f}{2} \frac{1}{I_{1s}E_{1s}} \frac{1}{\beta^3} \frac{\cos 2h\beta + \cosh 2h\beta + 2}{4 \sin 2h\beta + 4 \sinh 2h\beta} \tag{61}$$

if the definitions of the notations (55) and the values of the Krylov functions are also inserted.

This equation can be transformed further if we substitute β together with E_1 on the basis of $(2a)_2$ and $(2b)_2$

$$u_\zeta(\xi = 0) = u_{\zeta\,o} = -\frac{1}{I_{1s}E_{1s}} \frac{1}{\left(\nu_o \sqrt{\frac{R_e}{b_s} \frac{1}{R_e}} \right)^3} \frac{f_o - f}{8} \frac{\cos 2h\beta + \cosh 2h\beta + 2}{\sin 2h\beta + \sinh 2h\beta} =$$

$$= -\frac{\nu_o}{2E_s} \left(\frac{R_e}{b_s} \right)^{\frac{3}{2}} \frac{\cos 2h\beta + \cosh 2h\beta + 2}{\sin 2h\beta + \sinh 2h\beta} (f_o - f) . \tag{62}$$

1.3 Solution for the Second Partial Load

Comparing boundary condition $(5c)_1$ and relation $(54)_1$ we get

$$u_\zeta(\xi)|_{\xi=0} = a_1 = 0 . \tag{63}$$

Using boundary condition $(5c)_1$ and formula $(4)_2$ for the shear force in a similar manner we can write

$$-I_{1s}E_{1s}u_\zeta''|_{\xi=0} = -I_{1s}E_{1s}\beta^2 a_3 = -\frac{M_o}{2} , \qquad \text{i.e.} \qquad a_3 = \frac{M_o}{2} \frac{1}{I_{1s}E_{1s}} \frac{1}{\beta^2} . \tag{64}$$

The other two boundary conditions $(5d)_{1,2}$ yield the following system of linear equations

$$u_\zeta'''|_{\xi=h} = -4\beta^3 a_2 V_{3h} - 4\beta^3 \frac{M_o}{2} \frac{1}{I_{1s}E_{1s}} \frac{1}{\beta^2} V_{4h} + \beta^3 a_4 V_{1h} = 0 ,$$

$$u_\zeta''|_{\xi=h} = -4\beta^2 a_2 V_{4h} + \beta^2 \frac{M_o}{2} \frac{1}{I_{1s}E_{1s}} \frac{1}{\beta^2} V_{1h} + \beta^2 a_4 V_{2h} = 0 . \tag{65}$$

The solution are

$$\begin{bmatrix} a_2 \\ a_4 \end{bmatrix} = \frac{1}{I_{1s}E_{1s}} \frac{1}{\beta^2} \frac{M_o}{2} \begin{bmatrix} \dfrac{1}{4} \dfrac{V_{1h}^2 + 4V_{2h}V_{4h}}{V_{1h}V_{4h} - V_{2h}V_{3h}} \\ \dfrac{4V_{4h}^2 + V_{1h}V_{3h}}{V_{1h}V_{4h} - V_{2h}V_{3h}} \end{bmatrix} . \tag{66}$$

Making use of the solutions obtained for the integration constants (63), (64) and (65) we have from $(54)_1$ that

$$u_\zeta = \frac{1}{I_{1s}E_{1s}} \frac{1}{\beta^2} \frac{M_o}{2} \left(\frac{V_{1h}^2 + 4V_{2h}V_{4h}}{4V_{1h}V_{4h} - 4V_{2h}V_{3h}} V_2 + V_3 + \frac{4V_{4h}^2 + V_{1h}V_{3h}}{V_{1h}V_{4h} - V_{2h}V_{3h}} V_4 \right) . \tag{67}$$

Its derivative with respect to ξ is

$$\frac{du_\zeta}{d\xi} = \frac{1}{I_{1s}E_{1s}} \frac{1}{\beta^2} \frac{M_o}{2} \left(\beta \frac{V_{1h}^2 + 4V_{2h}V_{4h}}{4V_{1h}V_{4h} - 4V_{2h}V_{3h}} V_1 + \beta V_2 + \beta \frac{4V_{4h}^2 + V_{1h}V_{3h}}{V_{1h}V_{4h} - V_{2h}V_{3h}} V_3 \right) . \tag{68}$$

Substituting the definitions of the notations (55) and those of the Krylov functions together with the constants β and E_1 on the basis of $(2a)_2$, $(2b)_2$ we obtain the final form of the derivative

$$\left. \frac{du_\zeta}{d\xi} \right|_{\xi=0} = \frac{1}{I_{1s}E_{1s}} \frac{1}{\beta} \frac{M_o}{2} \frac{V_{1h}^2 + 4V_{2h}V_{4h}}{4V_{1h}V_{4h} - 4V_{2h}V_{3h}} = -\frac{1}{2I_{1s}E_{1s}} \frac{1}{\beta} \frac{\cos 2h\beta + \cosh 2h\beta + 2}{\sinh 2h\beta - \sin 2h\beta} M_o =$$

$$= -\frac{\nu_o^3}{E} \left(\frac{R_e}{b_s} \right)^{\frac{1}{2}} \frac{\cos 2h\beta + \cosh 2h\beta + 2}{\sinh 2h\beta - \sin 2h\beta} \frac{M_o}{b_s^2} . \tag{69}$$

17

1.4 Solution and Derivatives for Equation (21)

Here we present the linearly independent solutions $Z_1, \ldots, Z_4$ of the differential equation (21) together with their derivatives with respect to ρ

$$Z_1^{(o)} = Z_1 = 1\,, \qquad\qquad Z_1' = 0\,, \qquad Z_1'' = 0\,, \qquad Z_1''' = 0\,; \qquad (70a)$$

$$Z_2^{(o)} = Z_2 = \ln(\sqrt{\mathfrak{F}}\rho)\,, \qquad Z_2' = \frac{\sqrt{\mathfrak{F}}}{\sqrt{\mathfrak{F}}\rho} \qquad Z_2'' = -\frac{\mathfrak{F}}{\mathfrak{F}\rho^2}\,, \qquad Z_2''' = \frac{2\mathfrak{F}^{3/2}}{\mathfrak{F}^{3/2}\rho^3}\,; \qquad (70b)$$

$$Z_3^{(o)} = Z_3 = J_o(\sqrt{\mathfrak{F}}\rho)\,, \qquad\qquad Z_3' = -\sqrt{\mathfrak{F}}J_1(\sqrt{\mathfrak{F}}\rho)\,, \qquad (70c)$$

$$Z_3'' = \frac{\mathfrak{F}}{2}\left[J_2(\sqrt{\mathfrak{F}}\rho) - J_0(\sqrt{\mathfrak{F}}\rho)\right]\,, \qquad Z_3''' = -\frac{\mathfrak{F}^{3/2}}{4}\left[J_3(\sqrt{\mathfrak{F}}\rho) - 3J_1(\sqrt{\mathfrak{F}}\rho)\right]\,; \qquad (70d)$$

$$Z_4^{(o)} = Z_4 = Y_o(\sqrt{\mathfrak{F}}\rho)\,, \qquad\qquad Z_4' = -\sqrt{\mathfrak{F}}Y_1(\sqrt{\mathfrak{F}}\rho)\,, \qquad (70e)$$

$$Z_4'' = \frac{\mathfrak{F}}{2}\left[Y_2(\sqrt{\mathfrak{F}}\rho) - Y_0(\sqrt{\mathfrak{F}}\rho)\right]\,, \qquad Z_4''' = -\frac{\mathfrak{F}^{3/2}}{4}\left[Y_3(\sqrt{\mathfrak{F}}\rho) - 3Y_1(\sqrt{\mathfrak{F}}\rho)\right]\,. \qquad (70f)$$

References

Bryan, G. H.: On the stability of a plate under thrust in its own plane with applications to the buckling of the sides of a ship. *Proceedings of the London Mathematical Society*, s1-22(1), (1890), 54–67.

Burmeister, D.: Stability of a circular plate stiffened by a cylindrical shell under the assumption of non-axisymmetrical deformations. In: *Proceedings of the 4th International Conference Computational Mechanics and Virtual Engineering* (2011), 210-215.

Collatz, L.: *Eigenwertaufgaben mit technischen Anwendungen*. Nauka, Moskow (1968), Russian Edition.

Erdélyi, A.: *Higher Transcendental Functions*, vol. 1. Nauka, Moscow (1974), Russian Edition.

Frostig, Y.; Simitses, G. J.: Buckling of ring-stiffened multi-annular plates. *Computers & Structures*, 29, 3, (1988), 519–526.

Kozák, I.; Béda, G.: *Mechanics of elastic bodies*. Műszaki Könyvkiadó, Budapest (1987), (in Hungarian).

Nádai, A.: Über das Ausbeulen von kreisförmigen Platten. *Zeitschrift des Vereines deutscher Ingenieure*, 59, 11, (1915), 221–224.

Pardoen, G.: Vibration and buckling analysis of axisymmetric polar orthotropic circular plates. *Computers & Structures*, 4, (1974), 951–960.

Szilassy, I.: *Stability of circular plates with a hole loded on their outer boundary*. Ph.D. thesis, University of Miskolc (1971), (in Hungarian).

Szilassy, I.: Stability of an annular disc loaded on its external flange by an arbitrary force system. *Publ. Techn. Univ. Heavy Industry. Ser. D. Natural Sciences*, 33, (1976), 31–55.

Timoshenko, S.; Woinowski-Krieger, S.: *Theory of Plates and Shells*. McGraw-Hill, 2nd edn. (1987).

Turvey, G. J.; Der Avanessien, N. G. V.: Axisymmetric elasto-plastic large deflection response of ring siffened circular plates. *International Journal of Mechanical Sciences*, 31(11-12), (1989), 905–924.

Turvey, G. J.; Salehi, M.: Elasto-plastic large deflection response of pressure loaded circular plates stiffened by a single diameter stiffener. *Thin-Walled Structures*, 46, (2008), 996–1002.

Address: Dániel Burmeister, Department of Mechanics, University of Miskolc, 3515 Miskolc-Egyetemváros, Hungary

email: daniel.burmeister@uni-miskolc.hu